Thermal expansion of Ti_5Si_3 with Ge, B, C, N, or O additions

J.J. Williams, M.J. Kramer, and M. Akinc
Ames Laboratory and Department of Materials Science and Engineering, Iowa State University, Ames, Iowa 50011

(Received 3 August 1999; accepted 24 May 2000)

The crystallographic thermal expansion coefficients of Ti_5Si_3 from 20 to 1000 °C as a function of B, C, N, O, or Ge content were measured by high-temperature x-ray diffraction using synchrotron sources at Cornell University (Cornell High Energy Synchrotron Source; CHESS) and Argonne National Laboratory (Advanced Photon Source; APS). Whereas the ratio of the thermal expansion coefficients along the *c* and *a* axes was approximately 3 for pure Ti_5Si_3, this ratio decreased to about 2 when B, C, or N atoms were added. Additions of O and Ge were less efficient at reducing this thermal expansion anisotropy. The extent by which the thermal expansion was changed when B, C, N, or O atoms were added to Ti_5Si_3 correlated with their expected effect on bonding in Ti_5Si_3.

I. INTRODUCTION

Ti_5Si_3 displays a high melting point, low density, and with certain interstitial additions,[1] excellent oxidation resistance. However, the large thermal-expansion anisotropy of Ti_5Si_3 severely limits its practical use. This large anisotropy unavoidably causes the development of strain and microcracks during high-temperature synthesis and processing. Four previous studies have quantified the thermal-expansion anisotropy of Ti_5Si_3, three by high-temperature x-ray diffraction[2–4] and one by length-change measurements of a single crystal.[5] All studies measured a significantly larger expansion along the *c* axis compared to the *a* axis. The larger anharmonic vibration along the *c* axis was attributed to weak metallic bonding along this axis compared to strong covalent bonding along the *a* axis. This explanation is partly corroborated by electrical conductivity measurements that show the conductivity is twice as large along the *c* axis than along the *a* axis.[5]

Although all studies reported similar relative thermal expansions, the absolute values varied considerably (see Table I). Specifically, the standard deviation of measurement between the four studies was 9.7% for the coefficient of thermal expansion along the *c* axis (α_c) and 27% for the coefficient of thermal expansion along the *a* axis (α_a). One reason for the differences may be due to the presence of oxygen and nitrogen impurities. Based on reported lattice parameters, the Ti_5Si_3 synthesized by Ikarashi *et al.*[3] must have had approximately 1.0 wt% of oxygen, and the study by Thom *et al.*[4,6] suggests approximately 0.1 to 0.4 wt% of oxygen. The study by Williams *et al.*,[7] which systematically measured the change in lattice parameters of Ti_5Si_3 as a function of various interstitial additions, was used to estimate the impurity content. Due to similar effects on the lattice, nitrogen impurities may also be present. Regarding the remaining two studies, the lattice parameters reported by Zhang and Wu[2] were consistent with approximately 0.3 wt% excess silicon, and Nakashima and Umakoshi[5] did not report any lattice parameters.

One purpose of this study is to compare the effects that oxygen, nitrogen, carbon, and boron have on the thermal-expansion anisotropy of Ti_5Si_3. This may aid in explaining the scatter in the published values of supposedly pure Ti_5Si_3. A study by Thom *et al.*[4] did show that the addition of only 3.1 wt% carbon to Ti_5Si_3 increased α_a by 8% and decreased α_c by 12%. One important ramification of this study is that incorporation of carbon can reduce the thermal-expansion anisotropy of Ti_5Si_3, making it a more attractive engineering material. Furthermore, a similar result is expected for oxygen, nitrogen, and boron additions. The reason is that all of these atoms occupy the same interstice as carbon and all have similar effects on atomic separations and bonding within Ti_5Si_3. Unfortunately, the 20% reduction in thermal-expansion anisotropy as carbon is added to Ti_5Si_3 is not sufficient to avoid strain and microcracks during consolidation. A study by Kim *et al.*[8] modeled a maximum critical grain size needed to completely avoid microcracks for a given thermal-expansion anisotropy. Based on this model and the thermal-expansion coefficients from Thom *et al.*,[4] carbon-containing Ti_5Si_3 has a critical grain size of 5 to 6 μm, which is only a slight improvement over the critical grain size of 2 to 3 μm for pure Ti_5Si_3.

A more substantial reduction in thermal-expansion anisotropy has been reported in two studies, which replaced some of the titanium by zirconium, niobium, or chro-

mium.[2,3] Whereas carbon additions led to a 20% reduction in thermal-expansion anisotropy, zirconium substitutions yielded a 30% reduction and chromium a 70% reduction. According to Zhang and Wu,[2] very small quantities of niobium may actually reverse the thermal-expansion anisotropy, although further studies are necessary to substantiate this result. Another purpose of this study is to partially substitute silicon with germanium, because the effect that this type of compositional modification has on the thermal expansion has yet to be studied. The hope is that germanium substitutions will also reduce the thermal-expansion anisotropy, primarily by weakening the strong silicon–titanium network located in the basal planes.

II. EXPERIMENTAL PROCEDURE

Williams *et al.*[7] give a detailed description of sample synthesis and characterization. In summary, samples were synthesized by arc melting reagent-grade pieces of titanium and silicon/germanium with boron, graphite, TiN, or TiO_2 added to achieve the desired interstitial content. Weight losses were generally much less than 0.5 wt%, and synthesized samples were single phase. In addition, total carbon, nitrogen, and oxygen impurity content (Here impurity content refers to contamination by these elements, not intentional addition of C, N, or O.) was less than 0.09 wt% for all samples. Arc-melted samples for x-ray analysis were ground to <20 μm powder in an agate mortar.

Detailed descriptions of the sample furnace and diffractometer geometry are given by Margulies *et al.*[9,10] Diffraction experiments were run using 45 keV x-ray radiation. The high energy was necessary to achieve a negligible x-ray absorption by the furnace tube, as well as to provide diffraction by transmission rather than by reflection, which is the conventional method of high-temperature x-ray diffraction. Furthermore, an analyzer crystal of (111) Si was used before a NaI detector. The transmission geometry and analyzer crystal greatly reduce systematic and random errors associated with constantly shifting sample heights, a serious problem when using a conventional high-temperature diffractometer. However, the high x-ray energies that were used in this study significantly compress the measurable 2θ range of peak reflections. Thus, errors associated with calculations of lattice parameter are slightly larger. Specifically, the standard errors associated with lattice parameter refinements were approximately 0.001 Å.

The tube furnace used in the experiments, as described by Margulies *et al.*,[9,10] was designed such that thermal gradients across the sample were less than 1 °C. By comparison, vertical and horizontal thermal gradients of 50 to 100 °C are not uncommon for typical hot stages of conventional diffractometers. In addition, the sample thermocouple was calibrated against a National Institute of Standards and Technology (NIST) traceable thermocouple ensuring a measurement accuracy of better than 1 °C over the entire temperature range studied. Before heating, the furnace was purged with ultrahigh-purity-grade helium for at least 1 h, and a slow helium flow was maintained throughout the experiment. Diffraction scans were acquired from approximately 2° to 20° 2θ. The positions of 12 to 20 peaks were measured by fitting Pearson VII profiles to each peak, and the lattice parameters were calculated by a least-squares refinement program.[11] The 2θ zero and x-ray energy were calculated by adding silicon as an internal standard to the room-temperature scans.

TABLE I. Published values of linear coefficients of thermal expansion for Ti_5Si_3.

α_a, °C^{-1} × 10^{-6}	α_c, °C^{-1} × 10^{-6}	α_c/α_a	Reference
5.9 ± 0.2[a]	16.9 ± 0.6[a]	2.9 ± 0.2[a]	This study
6.3 ± 0.1[a,b]	17.8 ± 0.3[a,b]	2.8 ± 0.1[a]	Nakashima and Umakoshi[5]
8.7 ± 0.2[a]	22.1 ± 0.9[a,c]	2.5 ± 0.2[a]	Thom *et al.*[4]
10.4[d]	17.6[d]	1.7	Ikarashi *et al.*[3]
5.1	22.2	4.4	Zhang and Wu[2]

[a]Errors represent 90% confidence intervals.
[b]These thermal expansion coefficients were calculated by digitizing the plot given in Ref. 5.
[c]The α_c, as reported in Ref. 4 was incorrect. This is the correct value.
[d]These values were estimated from a bar chart.

III. RESULTS AND DISCUSSION

Figure 1 illustrates typical peak profiles obtained during this study. For one sample of Ti_5Si_3 and one of $Ti_5Si_3B_{0.5}$, each diffraction line was actually composed of two peaks—a sharp, intense peak accompanied by a weak, diffuse peak at a lower angle. This indicates that

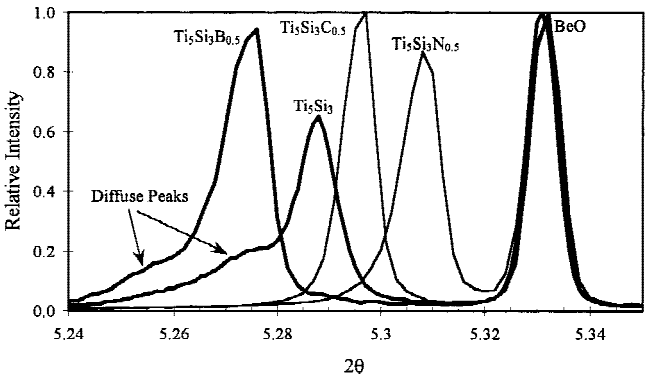

Fig. 1. Examples of peak profiles of $Ti_5Si_3Z_x$ obtained from synchrotron sources. Ti_5Si_3 and $Ti_5Si_3B_{0.5}$ were broader than samples with carbon, nitrogen, and oxygen and showed a diffuse low-angle tail. This indicates that a small portion of the Ti_5Si_3 and $Ti_5Si_3B_{0.5}$ samples was not well crystallized. The BeO peak is from the furnace tube.

these samples were heterogeneous such that a small portion of the arc-melted ingot was not well crystallized. In these cases, two peaks were fit to each reflection when calculating thermal expansion. Other Ti_5Si_3 samples, which were not used in this study, showed additional peaks associated with each reflection, also indicating heterogeneity. Note that diffraction patterns taken by conventional diffractometers with Cu K_α radiation could not resolve this convoluted peak structure due to inherently larger instrumental broadening compared to synchrotron sources and due to the added presence of the $K_{\alpha 2}$ peak.[9] In contrast, samples with carbon, nitrogen, and oxygen did not show a convoluted peak structure, which indicates well-crystallized and more homogeneous arc-melted ingots. This suggests that interstitial atoms may enhance ordering during the solidification process. Although boron also primarily resides in the same interstitial site, the fact that it does not follow this pattern suggests that boron may also partially substitute for silicon during solidification. Several silicides are known to exist where silicon atoms can be substituted with boron—$Mo_5(Si,B)_3$ is a common example. The reason that boron readily substitutes for silicon may be due to its larger size compared to carbon, nitrogen, and oxygen.

A summary of lattice parameters as a function of temperature is illustrated in Fig. 2. At least two data points were taken on cooling to compare with data taken on heating. In all cases but one, the lattice parameters obtained on cooling were within 0.002 Å of the lattice parameter obtained on heating ($Ti_5Si_3O_{0.4}$ being the exception had a 0.004 Å difference). This good agreement suggests the following: Samples did not significantly react with their surroundings, the diffractometer remained in alignment, and the synchrotron energy did not change significantly throughout the experiment. Thus, no significant systematic errors are anticipated in most of these measurements. The largest error in this study is expected to be the random error associated with the determination of lattice parameters, about ±0.002 Å. However, systematic errors associated with the measurement of germanium-containing samples could not be entirely precluded. Unlike the other samples whose spectra were taken with a 2θ step scan and NaI detector, the spectra of germanium-containing samples were collected with image plates. The difficulty in measuring the distance from the sample to the image plate as a function of the position of the image plate can lead to systematic errors.

Table II lists the thermal-expansion data of this study. The data assume linear thermal expansion along both crystallographic directions. The room-temperature lattice parameters listed in Table II were measured by a conventional diffractometer with NIST silicon (SRM 640b) added as an internal standard (see Williams *et al.*[7] for additional details). The synchrotron energy and diffractometer zero were refined until the measured room-temperature lattice parameters matched those listed in Table II. Only the data of Nakashima and Umakoshi[5] are consistent with the α's of Ti_5Si_3 as measured in this study. A comparison of the data is illustrated in Fig. 3. The small difference in α's between studies could be attributed to a slightly different oxygen content (lower in this study) and/or a 5% systematic error in temperature measurement. The α_c/α_a ratio reported by Thom *et al.*[4] for Ti_5Si_3 is most consistent with a sample containing oxygen, and the ratio for the carbon-containing sample is in excellent agreement with the carbon-containing samples of this study. However, the α's for each axis reported by Thom *et al.*[4] are consistently larger by 23 to 27% than the α's reported in this study. This suggests a relatively large systematic error that is very reproducible from sample to sample between these two measurement techniques—most likely an error in measuring the temperature. The differences between other studies are more

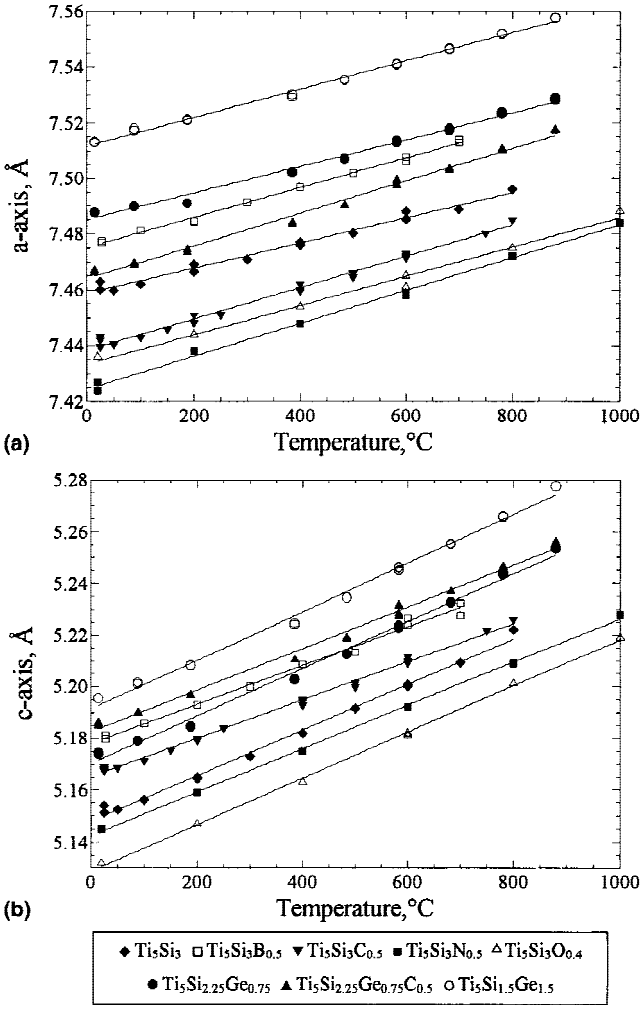

Fig. 2. (a) Expansion of the *a* axis and (b) *c* axis for all samples of this study. Lattice parameters as a function of temperature were calculated by least-squares refinement using the positions of 12 to 20 diffraction lines.

extreme and not easily explained. The results of Ikarishi *et al.*,[3] whose samples are thought to have a high oxygen content, qualitatively agree with the α's of $Ti_5Si_3O_{0.4}$; however, α_a is significantly larger than this study suggests. One reason may be a significant error associated with their method of calculating lattice parameters—simultaneous solution of two equations based on the positions of only two peaks. This method of calculation is much less accurate than the typical least-squares technique. Finally, the results of Zhang and Wu[2] are inconsistent with this and every other study.

The interstice that boron, carbon, nitrogen, and oxygen occupy is formed by six titanium atoms in an octahedral configuration. These octahedra are face shared along the *c* axis. In pure Ti_5Si_3, most of the bonding along the *c* axis is thought to be due to this chain of face-shared octahedra of titanium atoms as well as a linear chain of titanium atoms parallel to the octahedral chain. Furthermore, the bonding associated with the linear chain is expected to be stronger than the bonding associated with the octahedral chain. On addition of interstitial atoms, the weak bonding associated with the octahedral chain is replaced by stronger titanium–interstitial-atom bonding. Whereas the weak titanium–titanium-octahedral bonds are primarily directed along the *c* axis, the titanium–interstitial-atom bonds have nearly equal components along the *a* and *c* axes. Thus, as carbon is added to Ti_5Si_3, for example, the α_c decreases due to replacement of weak metallic bonds with stronger covalent bonds. However, the anharmonic vibrations of these titanium–carbon bonds are large enough to increase the total α_a.

Comparison of α's in other compounds gives an indication of why α_a is increasing as interstitial atoms are added to Ti_5Si_3. The α of TiC, a compound composed solely of titanium–carbon bonds, is approximately 7.95×10^{-6} °C^{-1} and the α of TiN is approximately 8.2 to 9.1×10^{-6} °C^{-1}.[12] Both values are significantly larger than the α_a of pure Ti_5Si_3. Thus, α_a increases as carbon and nitrogen are added to Ti_5Si_3 such as to approach the magnitude of anharmonic vibrations seen in TiC and TiN. Also, based on sublimation energies of TiZ compounds (Z = B, C, N, or O), one would expect titanium–carbon bonds to be the strongest and titanium–oxygen bonds the weakest. Furthermore, whereas the titanium–carbon separation in Ti_5Si_3 is similar to the separation in TiC, the titanium–oxygen separations are significantly longer. For these reasons, addition of carbon to Ti_5Si_3 has a significantly stronger influence on the α's than does addition of oxygen.

By comparing the properties of silicides to the properties of their germanide counterparts, one expects weaker, more anharmonic bonding in the germanides. Thus, partial substitution of silicon with germanium was expected to increase the overall thermal-expansion coefficient. Additionally, because most of the titanium–silicon/germanium bonding is expected to fall in the (001) planes, a larger increase in α_a than α_c was expected. This study does show this assertion to be true. For example, $Ti_5Si_{1.5}Ge_{1.5}$ shows a 13.3% increase in α_a accompanied by only a 7.6% increase in α_c. Unfortunately, this leads to a relatively insignificant change in the thermal-expansion anisotropy. Thus, substitution for silicon atoms is not a viable method of reducing the thermal-expansion anisotropy.

Based on the crystallographic α's, bounds of the bulk thermal expansion, α_{bulk}, as derived by Hashin[13] can be determined by

$$\alpha_{bulk} = (2\alpha_a + \alpha_c)/3 \quad , \tag{1}$$

$$\alpha_{bulk} = (2\alpha_a + \alpha_c)/3 + 2\Psi\,(\alpha_a - \alpha_c)/3 \quad . \tag{2}$$

Equation (1) is based on the Reuss approximation of the bulk elastic modulus, Eq. (2) is based on the Voight approximation, and Ψ is a function of the compliance tensor only. These bounds assume a random distribution of uniform grains such that the bulk material is statistically

TABLE II. Room-temperature lattice parameters and linear coefficients of thermal expansion from room temperature to 1000 °C.

		Å, 25 °C		°$C^{-1} \times 10^{-6}$		
Sample	Source	a^a	c^a	$\alpha_a{}^b$	$\alpha_c{}^b$	$\alpha_c/\alpha_a{}^b$
Ti_5Si_3	APS	7.4591 (1)	5.1515 (1)	5.8 ± 0.6	17.0 ± 2.2	2.9 ± 0.7
Ti_5Si_3	CHESS	7.4600 (2)	5.1517 (1)	6.0 ± 0.2	17.0 ± 0.4	2.8 ± 0.2
$Ti_5Si_3B_{0.5}$	CHESS	7.4782 (1)	5.1788 (1)	7.2 ± 0.3	14.5 ± 0.8	2.0 ± 0.2
$Ti_5Si_3C_{0.5}$	CHESS	7.4399 (1)	5.1677 (1)	7.6 ± 0.2	14.3 ± 0.5	1.9 ± 0.1
$Ti_5Si_3C_{0.5}$	APS	7.4415 (1)	5.1687 (1)	7.3 ± 0.3	14.1 ± 0.6	1.9 ± 0.2
$Ti_5Si_3C_{0.85}$	Thom *et al.*[4]	7.4438 (4)	5.1643 (4)	9.3 ± 0.4	17.9 ± 1.3	1.9 ± 0.2
$Ti_5Si_3N_{0.5}$	APS	7.4273 (1)	5.1453 (1)	7.9 ± 0.4	16.3 ± 0.4	2.1 ± 0.2
$Ti_5Si_3O_{0.4}$	APS	7.4342 (1)	5.1334 (1)	7.0 ± 0.7	17.4 ± 0.6	2.5 ± 0.3
$Ti_5Si_{2.25}Ge_{0.75}$	CHESS	7.4868 (1)	5.1743 (1)	6.4 ± 0.3	17.8 ± 0.5	2.8 ± 0.2
$Ti_5Si_{2.25}Ge_{0.75}C_{0.5}$	CHESS	7.4664 (1)	5.1859 (1)	7.9 ± 0.3	15.6 ± 0.5	2.0 ± 0.1
$Ti_5Si_{1.5}Ge_{1.5}$	CHESS	7.5140 (2)	5.1964 (1)	6.8 ± 0.2	18.3 ± 0.6	2.7 ± 0.2

[a]Values in parentheses represent the standard error of the lattice parameter calculation.
[b]Errors represent 90% confidence intervals.

homogeneous. Because the compliance tensor for Ti_5Si_3 has not been measured, Fig. 4 illustrates estimates for α_{bulk} based only on Eq. (1). Nitrogen, oxygen, and germanium additions significantly increase the bulk thermal expansion coefficient of Ti_5Si_3. Thus, these elements would be most efficient at tailoring the bulk thermal expansion to a given application.

Reported values of the bulk thermal expansion of Ti_5Si_3, as measured by dilatometry, show very large deviations between studies.[4,14,15] One reason is due to the presence of impurities because typical powder-processing routes can lead to significant amounts of interstitial carbon, nitrogen, and oxygen. However, another major reason in the scatter may be due to the presence of microcracks and residual strain that will form because of the thermal-expansion anisotropy. The magnitude of these effects will strongly depend on the processing method (e.g., hot pressing versus pressureless sintering).

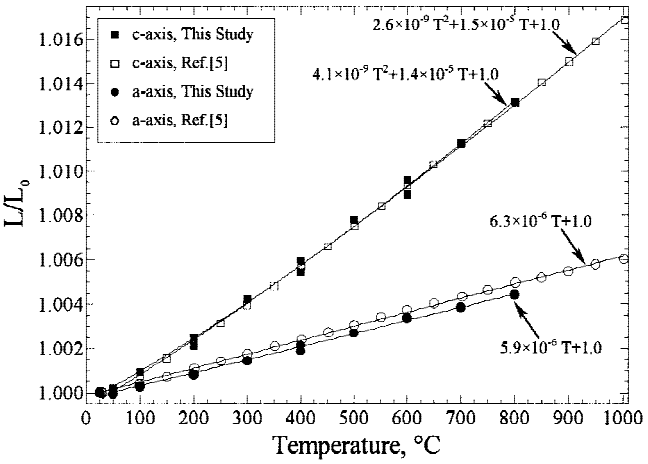

Fig. 3. Thermal expansion of Ti_5Si_3 as measured in this study compared to the thermal expansion measured by Nakashima and Umakoshi.[5] Note that both residual analysis and lack of fit tests suggest that the expansion of the *c* axis is best fit by a quadratic equation. However, this study reports only linear expansion because the standard errors associated with the quadratic coefficient were large, 50–100%. Much finer temperature increments are needed to get an accurate estimate of this curvature. In contrast, the expansion of the *a* axis over the studied temperature range of 25 to 1000 °C is best fit by a linear equation.

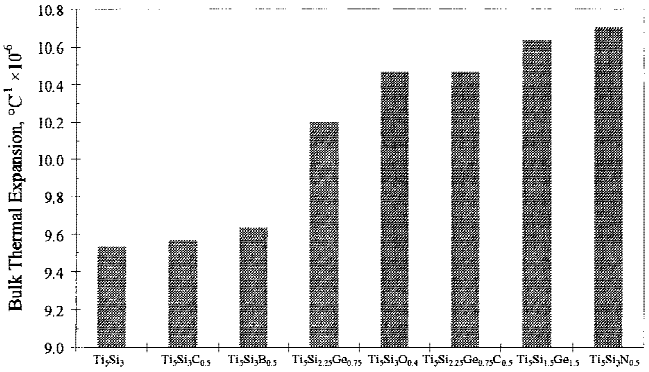

Fig. 4. Estimated bulk thermal-expansion coefficient based on the crystallographic thermal-expansion coefficients α_a and α_c.

IV. CONCLUSIONS

This study suggests that some of the scatter in published values of thermal-expansion coefficients of Ti_5Si_3 can be explained by oxygen impurities. However, systematic errors must also exist in some or all of the studies, although this study did attempt to minimize these errors. The most probable reasons for discrepancies between studies are inaccurate temperature measurements, shifting sample heights, and reactions on the surface of the samples associated with x-ray-diffraction experiments.

In agreement with a previous study, this study has shown that carbon additions, as well as boron, nitrogen, and oxygen additions, do reduce the thermal-expansion anisotropy of Ti_5Si_3 by as much as 34%. Reduction of this anisotropy is necessary to produce a strain-free and crack-free microstructure. Unfortunately, substitutions for silicon atoms or incorporation of interstitial atoms alone are not sufficient to entirely eliminate the thermal-expansion anisotropy. However, these compositional modifications may be an effective method of tailoring the bulk thermal expansion to a given application.

ACKNOWLEDGMENTS

The authors acknowledge the hard work of Dr. Stefan Kycia of the Cornell High Energy Synchrotron Source (CHESS) and Dr. Dean Haeffner of the Advanced Photon Source (APS) in setting up and aligning the equipment associated with the synchrotron sources. The authors also acknowledge Larry Margulies for help in data acquisition, and Dr. Andrew Thom for useful discussions. Ames Laboratory is operated for the U.S. Department of Energy by Iowa State University under Contract Number W-7405-ENG-82. The APS is supported by the U.S. Department of Energy, Basic Energy Sciences–Materials Sciences, under Contract No. W-31-109-ENG-38. The CHESS is supported by the National Science Foundation under Award No. DMR-9311772.

REFERENCES

1. A.J. Thom and M. Akinc, in *Advanced Ceramics for Structural and Tribological Applications,* edited by H.M. Hawthorne and T. Troczynski (Metallurgical Society of Canadian Institute of Mining, Metallurgy and Petroleum International Symposium Proceedings, Vancouver, BC, Canada, 1995), p. 619.
2. L. Zhang and J. Wu, Scripta Mater. **38,** 307 (1998).
3. Y. Ikarashi, K. Ishizaki, T. Nagai, Y. Hashizuka, and Y. Kondo, Intermetallics **4,** 141 (1996).

4. A.J. Thom, M. Akinc, O.B. Cavin, and C.R. Hubbard, J. Mater. Sci. Lett. **13,** 1657 (1994).
5. T. Nakashima and Y. Umakoshi, Philos. Mag. Lett. **66,** 317 (1992).
6. A.J. Thom, V.G. Young, and M. Akinc, J. Alloys Compds. **296,** 59 (2000).
7. J.J. Williams, M.J. Kramer, M. Akinc and S.K. Malik, J. Mater. Res. **15,** 99–335 (2000).
8. Y. Kim, A.J. Thom, and M. Akinc, in *Processing and Fabrication of Advanced Materials for High Temperature Applications–II,* edited by T.S. Srivatsan and V.A. Ravi (The Minerals, Metals and Materials Society Symposium Proceedings, Warrendale, PA, 1992), p. 189.
9. L. Margulies, M.J. Kramer, J.J. Williams, E.M. Deters, R.W. McCallum, D.R. Haeffner, J.C. Lang, S. Kycia, and A.I. Goldman, in *Applications of Synchrotron Radiation Techniques to Materials Science IV,* edited by S.M. Mini, S.R. Stock, D.L. Perry, and L.J. Terminello (Mater. Res. Soc. Symp. Proc. **524,** Warrendale, PA, 1998), p. 139.
10. L. Margulies, M.J. Kramer, R.W. McCallum, S. Kycia, D.R. Haeffner, J.C. Lang, and A.I. Goldman, Rev. Sci. Instrum. **70,** 3554 (1999).
11. D.E. Appleman and H.T. Evans, U.S. National Technical Information Service, Document No. PB2-16188 (1973).
12. *Carbide, Nitride and Boride Synthesis and Processing,* edited by A.W. Weimer (Chapman and Hall, London, 1997), p. 646.
13. Z. Hashin, J. Mech. Phys. Solids **32,** 149 (1984).
14. R. Mitra, Metall. Mater. Trans. A **29,** 1629 (1998).
15. R. Rosenkranz, G. Frommeyer, and W. Smarsly, Mater. Sci. Eng., A **152,** 288 (1992).